engineering proceedings

MDPI

Proceeding Paper

Design, Modelling and Simulation of Fault Behavior in Hybrid Multiterminal HVDC Collection Systems †

Olumoroti Ikotun *, Evans Eshiemogie Ojo and Musasa Kabeya

Department of Electrical Power Engineering, Durban University of Technology, Durban 4001, South Africa; evanso@dut.ac.za (E.E.O.); musasak@dut.ac.za (M.K.)

* Correspondence: 22494799@dut4life.ac.za

† Presented at the 34th Southern African Universities Power Engineering Conference (SAUPEC 2026), Durban, South Africa, 30 June–1 July 2026.

Abstract

Previous studies showed that at the inverter end, the AC voltage will experience a slight increase, while further observations revealed an increase in DC current. Other findings indicated that the AC voltage at the rectifier side will experience a decrease, while both AC voltage and DC current will increase. This paper presents a hybrid multiterminal HVDC system, which was modelled and implemented using Matlab/Simulink software 2018b to investigate fault behaviors, focusing on DC line-to-ground faults and their impact on the overall system. Calculations were performed at the input of the Graetz bridge rectifier, the capacitor filter of the DC transmission line, and the three-phase LCL filter located at the inverter end. Results indicated that, at the rectifier end, the grid voltage will increase while the grid current will decrease with non-standard waveforms. It noted that at the inverter end, the AC voltage will decrease along with grid currents. In the DC transmission line, the DC current will decrease to near zero. Findings represent the contribution of the behaviors observed at both the rectifier and inverter ends of the grids during fault scenarios, providing a more profound understanding of how multiterminal HVDC systems behave under threat.

Keywords: hybrid multiterminal HVDC; DC line-to-ground fault; Matlab/Simulink software; inverter side; rectifier side; simulation

1. Introduction

The increased demand for sustainable energy, coupled with the need for efficient electricity transmission systems, has led to the development of advanced technologies in high-voltage direct current (HVDC) systems. Among these innovations are hybrid multiterminal HVDC systems, which provide numerous advantages over traditional AC systems, including increased transmission capacity, reduced energy losses, and enhanced system reliability. Despite their advantages, hybrid MT-HVDC collection systems are susceptible to various faults [1]. Faults can lead to significant operational challenges and impact the reliability of the entire electricity network. For example, in an investigation published by Yuan and Cheng [2], they explored the activities of the inverter side during a DC line-to-ground fault, finding that the AC voltage experienced a slight increase. This assertion proceeds to highlight a vital aspect of voltage behavior in hybrid systems that merits further examination within the broader context of ongoing research. Conversely, Torres-Olguin and Garces [3] disputed this position, asserting that the AC voltage at the inverter

Check for updates

Academic Editor: Akshay Kumar Saha

Published: 14 May 2026

Copyright: © 2026 by the authors. Licensee MDPI, Basel, Switzerland. This article is an open access article distributed under the terms and conditions of the Creative Commons Attribution (CC BY) license.

side will indeed fall to zero under similar fault conditions. This contention introduces critical dimensions to the discourse on faulty behavior in multiterminal HVDC systems, showcasing the necessity for investigations into these opposing claims. Elgeziry et al. [4] contributed further to the discussion by analyzing the behavior of voltage and current at the rectifier side of the system during line-to-ground fault. They contended that the AC voltage at this juncture will experience a decrease, while concurrently, both the AC and DC currents will demonstrate an increase. The identification of this dual behavior is vital for understanding the overall system response and how fault conditions can affect the efficiency and safety of multiterminal HVDC operations. Indeed, the assertion made by Elgeziry et al. [4] is corroborated by a series of studies that reinforce their findings regarding the increase in DC current. Yang et al. [5], Mond et al. [6], Kaur et al. [7], and Düllmann et al. [8] collectively validated the hypothesis that the magnitude of the DC current will rise significantly during such fault conditions. Düllmann et al. [8] further augmented this discourse by noting that the DC voltage will simultaneously experience an increase, adding another layer to the system's behavior during faulty conditions. In addition, Troitzsch et al. [9] contributed to the discourse by underscoring that any fault occurring in proximity to the converter can precipitate a substantial increase in current, thus enhancing the understanding of spatial factors that must be accounted for in system design and fault analysis. While these studies add to the understanding of multiterminal HVDC systems during DC line-to-ground faults, a closer inspection raises concerns about the completeness and coherence of the existing data, particularly concerning the DC current, the grid voltage rectifier end; the inverter side of both grid voltage and current during fault conditions remains inadequately addressed, and this will be addressed in this paper.

2. Materials and Methods

A hybrid multiterminal HVDC system has been developed, and various parameters, including the capacitor filter for the DC transmission line, the input voltage for the Graetz bridge rectifier, and the three-phase LCL filter, have been computed. In Figure 1, is a proposed diagram illustrating a hybrid multiterminal HVDC system.

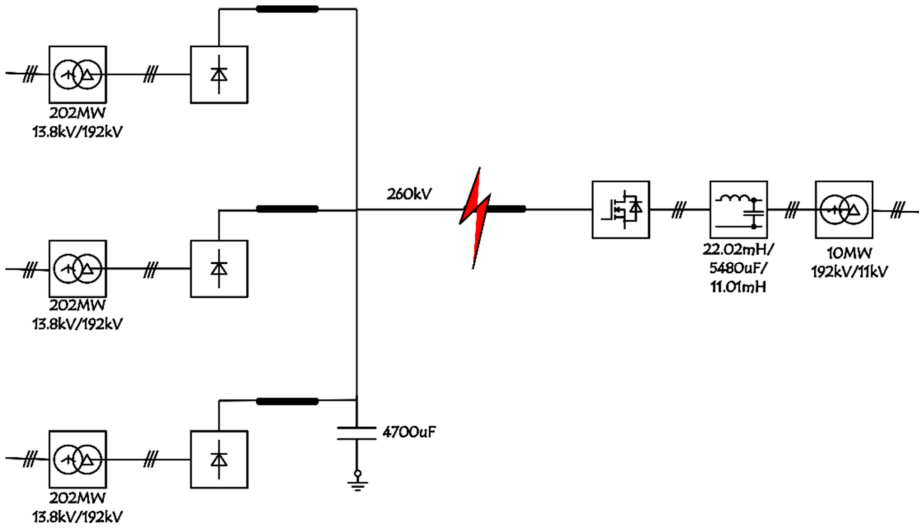


Figure 1. Block diagram of a proposed hybrid multiterminal HVDC system.

2.1. Six-Pulse Graetz Bridge

The six-pulse Graetz bridge [10] is a significant structure within power electronics primarily utilized for converting alternating current (AC) to direct current (DC) [11,12]. The bridge configuration consists of (D_1 to D_6). (D_1, D_3, D_5) (top group) is connected to the

positive terminal and (D_2, D_4, D_6) (bottom group) is connected to the negative terminal. Each diode conducts for 1/3 of a cycle. The average output DC voltage is derived from the line-to-line voltage, and the equation is defined by the formula, and it also accounts for the diode forward voltage drop $\left(V_{dropD}\right)$ and the equation is given as follows:

$$V_{dc} = \left(\frac{3\sqrt{2}}{2} V_{LL(rms)}\right) - 2V_{dropD} \quad (1)$$

The secondary output of the transformer is provided which represents as line-to-line RMS voltage $\left(V_{LL(rms)}\right)$:

$$V_{dc} = \left(\frac{4.2426}{\pi} \times 192,525\right) - 2V_{dropD} = (1.350 \times 192,525) - 2V_{dropD}.$$

The $2V_{dropD}$ was neglected and the DC voltage value $V_{dc} = 259,999.2 \approx 260$ kV. However, in the DC line voltage, it requires a capacitor (C_{filter}) to filter the unwanted noise, and the equation is given as follows:

$$C_{filter} = \frac{I_{currLoad}}{2 \times f_{ripple} \times V_{allow.Ripple}} \quad (2)$$

where the $I_{currLoad}$ represent the load current, f_{ripple} is the ripple frequency, and $V_{allow.Ripple}$ which refers to the ripple voltage. The ripple frequency for a 60 Hz Graetz bridge and desired ripple of 1% are given in the equation:

$$C_{filter} = \frac{2624.3}{2 \times 60 \times 6500} \times 10^6 = 3364 \approx 4700 \text{ uF}.$$

2.2. Three-Phase LCL Filter

LCL filters are passive components composed of two inductors and a capacitor, connected in a way that attenuates high-frequency harmonics from the output signal of the inverter [13–15]. They serve to mitigate the effects of high-frequency noise produced during the switching actions of the inverter which, without proper filtering, could lead to resonance issues and overheating of connected equipment. To ensure ripple attenuation and system stability, the equation and exact calculation are given. The base impedance ($Z_{base.Inv}$) and the rated current (I_{rated_Inv}) are considered in this equation:

$$Z_{base.Inv} = \frac{V_{L-L_Inv}^2}{S_{Inv}} = \frac{11000^2}{50 \times 10^6} = 2.42\ \Omega,$$

$$I_{rated_Inv} = \frac{S_{Inv}}{\sqrt{3} V_{L-L_Inv}} = \frac{50 \times 10^6}{\sqrt{3} \times 11000} \approx 2624.3 \text{ A}.$$

At the inverter side inductor (L_{Inv}) was sized to maintain the current ripple (ΔI_{L_Inv}) in a limited range while the15% of the peak current was used in this study. The maximum ripple current is given as follows:

$$\Delta I_{max_Inv} = 0.15 \times I_{rated_Inv} = 0.15 \times 2624.3 \approx 393.6 \text{ A}.$$

However, the equation of the inductance (L_{Inv}) at the inverter side is given as follows:

$$L_{Inv} = \frac{V_{dc}}{6 \times f_{sw_Inv} \times \Delta I_{max_Inv}} = \frac{260000}{6 \times 5000 \times 393.6} \approx 22.02 \text{ mH}$$

For the filter capacitor (C_{f_Inv}), it was at capped at 5% (0.05) of the power to maintain a high-power factor. The base capacitance was first considered as follows:

https://doi.org/10.3390/engproc2026140019

$$C_{base_Inv} = \frac{1}{\omega_{grid.f_Inv} \times Z_{base.Inv}} = \frac{1}{2\pi \times 60 \times 2.42} \approx 1.096 \text{ mF}$$

$C_{f_Inv} = 0.005 \times C_{base_Inv} = 0.005 \times 0.001315 \Rightarrow 10^6 \times 0.005 \times 0.001315 = 5.480$ µF. At the grid side inductor $L_{grid_Inv} = 0.5L_{Inv} = 0.5 \times 22.02 \approx 11.01$ mH. Furthermore, the damping resistor (R_{d_Inv}) was used in series with the filter capacitor to prevent the undesired resonance frequency, written as follows:

$$R_{d_Inv} \approx \frac{1}{3 \times 2\pi f_{res.Inv} \times C_{f_Inv}} \tag{3}$$

$$f_{res.Inv} = \frac{1}{2\pi}\sqrt{\frac{L_{Inv} + L_{grid_Inv}}{L_{Inv}L_{grid_Inv}C_{f_Inv}}} = \frac{1}{2\pi}\sqrt{\frac{33.03 \text{ mH}}{242.440 \text{ mH} \times 5.480 \text{ µF}}} = 793.6 \text{ Hz}.$$

To prevent instability and ensure attenuation the frequency must be between the grid and switching frequencies range $\left(10 \times f_{grid_Inv} \text{ and } 0.5 \times f_{sw_Inv}\right)$. However, both the L_{Inv} and C_{f_Inv} were not adjusted in the simulation to shift resonance. The resonance frequency stayed within the range.

$$R_{d_Inv} \approx \frac{1}{3 \times 2\pi \times 793.6 \times 5.480 \times 10^{-6}} \approx 12\ \Omega$$

2.3. HVDC Transmission Line

HVDC technology is instrumental in transmitting electricity over long distances with reduced losses [16–18]. HVDC maintains a constant voltage and allows for higher transmission capacity over extended distances. To calculate the HVDC transmission distance, one must consider multiple factors, the type of conductors, environmental conditions, and system loss [19]. For overhead lines, the straight-line distance between towers is not the actual cable length due to sag caused by gravity and thermal expansion. The cable length equation is given as follows [20]:

$$L = \left(\frac{2 \times \sigma_{l_0}}{\gamma_{Cond_L}} \times \sinh\left(\frac{\gamma_{Cond_L} \times l}{2 \times \sigma_{l_0}}\right)\right) \times \sqrt{1 + h^2} \tag{4}$$

where σ_{l_0} is the horizontal stress at the lowest point of the conductor, γ_{Cond_L} is the specific load of the conductor, l is the span between towers, and h is the height difference between towers.

3. Simulation of the Hybrid Multiterminal HVDC System

To substantiate the preceding analysis, a simulation is conducted using Matlab/Simulink software R2018b under the assumption of a DC line-to-ground fault that transpires at the location shown in Figure 2. Parameters of the circuit have already been calculated in the materials and methods.

https://doi.org/10.3390/engproc2026140019

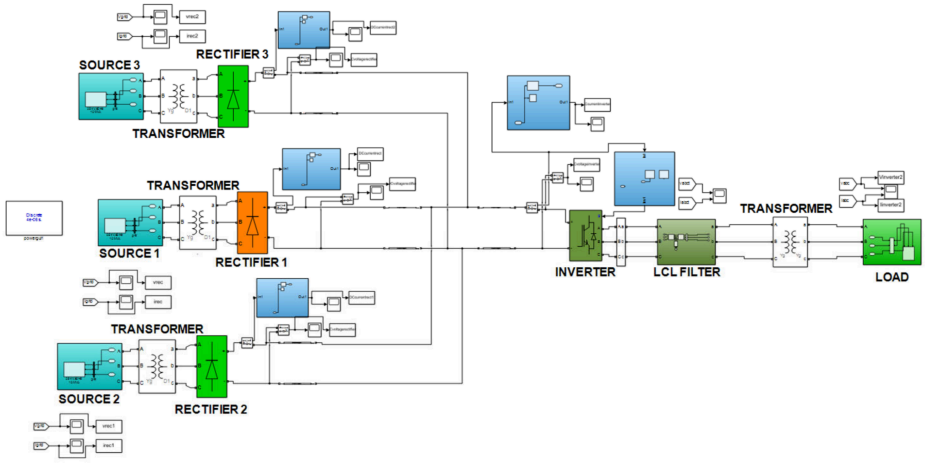


Figure 2. Model of the hybrid multiterminal HVDC system.

4. Results and Discussion

The operational reliability of a hybrid multiterminal HVDC collection system is continually challenged by faults, particularly during critical disturbances such as DC line-to-ground faults. In this paper, fault was deliberately induced in the DC transmission line for a duration of two to three seconds in Matlab/Simulink software R2018b, providing insights into the system's response under adverse conditions. During a DC line-to-ground fault, the dynamics at the rectifier end of the system are affected. The grid voltages will experience a gradual increase due to the fault with the electrical characteristics of the phases A, B, and C and will exhibit a marked decrease with non-standard waveforms in grid current shown in Figure 3. These changes will lead to the generation of distorted waveforms, which will deviate from the sine wave shapes expected in stable operating conditions, and this will negatively impact the quality of power if not appropriately addressed. In the DC transmission line, changes will occur during the DC line-to-ground fault. The DC voltage will tend to rise gradually; meanwhile, the DC link current will experience a significant reduction, approaching near zero levels as shown in Figure 4. At the inverter end of the system, the consequences of a line-to-ground fault will further complicate the operational scenario. It will be observed that there is a decrease in grid voltages, reflecting the stress imposed by the fault condition. Similar to the rectifier end, the inverter end will also experience diminishing grid current shown in Figure 5. The incomplete standard at this end underscores the instability that characterizes the system during faulty conditions. Nevertheless, an unanswered question remains: Can we achieve the same results if the design and experimental setup are used? The answer to this question can form the focus of another paper.

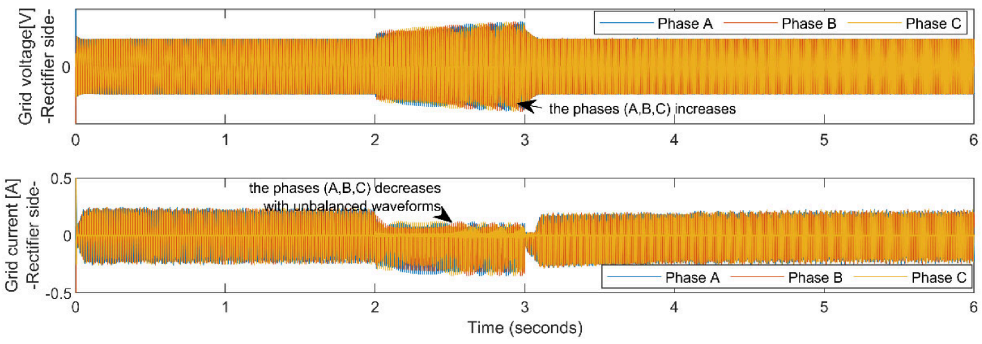


Figure 3. Grid voltages and currents at the rectifier end.

https://doi.org/10.3390/engproc2026140019

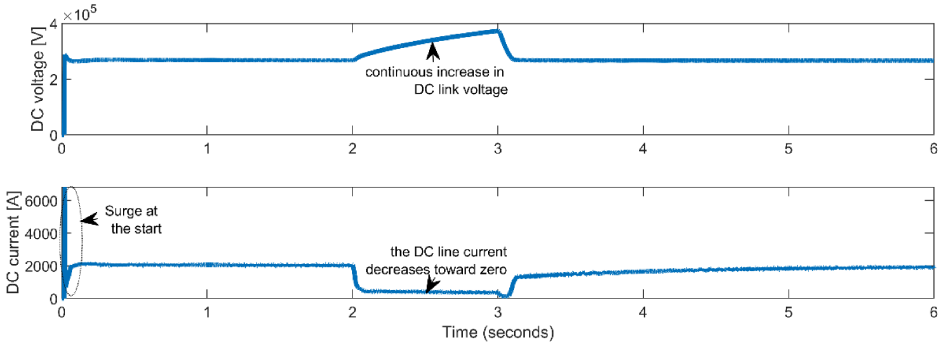


Figure 4. DC voltage and DC current.

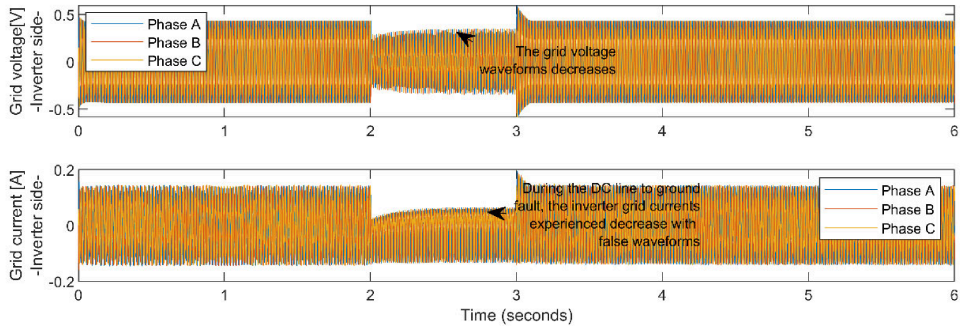


Figure 5. Grid voltages and currents at the inverter end.

5. Conclusions

In this study, a multiterminal HVDC system was modelled and implemented using Matlab/Simulink software to investigate the dynamics of a DC line-to-ground fault. Parameters such as the capacitor filter of the DC transmission line, the input voltage for the Graetz bridge rectifier, and the three-phase LCL filter were calculated and incorporated into the model. The simulation resulted in valuable insights into the system's behavior under stress, specifically a DC line-to-ground fault condition. The results revealed that, at the rectifier end, the grid voltage will tend to rise while the grid current will diminish with non-standard waveforms. Conversely, at the end of the inverter, both the AC voltage and grid currents will experience a decline. Additionally, the DC transmission line will show a significant reduction in DC current, approaching zero. These findings highlight the dynamics experienced at both the rectifier and inverter ends of the grid during fault scenarios, thereby enhancing our understanding of how multiterminal HVDC systems will respond under threat.

Author Contributions: Conceptualization, O.I., E.E.O. and M.K.; methodology, O.I., E.E.O. and M.K.; software O.I., E.E.O. and M.K.; validation, O.I., E.E.O. and M.K.; formal analysis, O.I., E.E.O. and M.K.; investigation, O.I., E.E.O. and M.K.; resources, O.I., E.E.O. and M.K.; data curation, O.I., E.E.O. and M.K.; writing—original draft, O.I.; writing—review and editing, O.I., E.E.O. and M.K.; visualization, O.I., E.E.O. and M.K.; supervision, O.I., E.E.O. and M.K.; project administration, O.I., E.E.O. and M.K.; funding acquisition, E.E.O. All authors have read and agreed to the published version of the manuscript.

Funding: This is funded by Durban University of Technology (DUT), directorate for research and postgraduate support.

Institutional Review Board Statement: Not applicable.

Informed Consent Statement: Not applicable.

Data Availability Statement: The contributions outlined in this study are detailed within the article. For additional questions, please reach out to the corresponding author.

Conflicts of Interest: The authors declare no conflicts of interest.

References

1. Anwar, T.; Mu, C.; Yousaf, M.Z.; Khan, W.; Khalid, S.; Hourani, A.O.; Zaitsev, I. Robust fault detection and classification in power transmission lines via ensemble machine learning models. *Sci. Rep.* **2025**, *15*, 2549. [CrossRef] [PubMed]
2. Yuan; Cheng. Simulation study for a hybrid multi-terminal HVDC system. In *Proceedings of 2005/2006 IEEE/PES Transmission and Distribution Conference and Exhibition*; IEEE: Piscataway, NJ, USA, 2006; pp. 720–725.
3. Torres-Olguin, R.E.; Garces, A. Grid Integration of offshore wind farms using a Hybrid HVDC composed by an MMC with an LCC-based transmission system. *Energy Procedia* **2017**, *137*, 391–400. [CrossRef]
4. Elgeziry, M.; Elsadd, M.; Elkalashy, N.; Kawady, T.; Taalab, A.M.; Izzularab, M.A. Non-pilot protection scheme for multi-terminal VSC–HVDC transmission systems. *IET Renew. Power Gener.* **2019**, *13*, 3033–3042. [CrossRef]
5. Yang, R.; Fang, K.; Chen, J.; Chen, Y.; Liu, M.; Meng, Q. A novel protection strategy for single pole-to-ground fault in multi-terminal dc distribution network. *Energies* **2023**, *16*, 2921. [CrossRef]
6. Mond, M.A.; Li, Z.; Mei, W. Modeling, Analysis, and Classification of Asymmetrical DC Faults in a Bipolar Hybrid Cascaded Multi-Terminal HVDC System. *Symmetry* **2025**, *17*, 1671. [CrossRef]
7. Kaur, J.; Jayasooriya, M.; Iqbal, M.N.; Daniel, K.; Shabbir, N.; Peterson, K. Fault Detection and Protection Strategy for Multi-Terminal HVDC Grids Using Wavelet Analysis. *Energies* **2025**, *18*, 1147. [CrossRef]
8. Düllmann, P.; Klein, C.; Winter, P.; Köhler, H.; Steglich, M.; Teuwsen, J.; Leterme, W. Preventive DC-side decoupling: A system integrity protection scheme to limit the impact of DC faults in offshore multi-terminal HVDC systems. *IET Gener. Transm. Distrib.* **2024**, *18*, 3801–3816. [CrossRef]
9. Troitzsch, C.; Marten, A.K.; Westermann, D. Non-telecommunication based DC line fault detection methodology for meshed HVDC grids. *IET Gener. Transm. Distrib.* **2016**, *10*, 4231–4239. [CrossRef]
10. Tavanaee, M.; Girona-Badia, J.; Cheah-Mañe, M.; Gomis-Bellmunt, O.; Prieto-Araujo, E. Grid-connected power converters for electrolysis applications. *IEEE Access* **2025**, *13*, 187211–187225. [CrossRef]
11. Wang, Y.; Luo, S.; Yu, M.; Yang, L.; Huang, J.; Huang, Z. Review of Lightweight Oriented Offshore Wind Power Transmission Schemes. *Chin. J. Electr. Eng.* **2025**, *11*, 16–39. [CrossRef]
12. Saadeh, M.; Hamdan, M.; Saadeh, O. Modelling and control of LCL voltage source converter-based hybrid high voltage alternating current/high voltage direct current system. *Int. J. Electr. Comput. Eng. (IJECE)* **2025**, *15*, 1297–1321. [CrossRef]
13. Jiang, J.; Wang, H.; Pan, S.; Liu, F.; Zhao, E.; Liu, G. Three-Phase Fully Magnetically Integrated LCL Filters with Enhanced Ripple Attenuation Capability. *IEEE J. Emerg. Sel. Top. Power Electron.* **2025**, *13*, 7993–8006. [CrossRef]
14. Koffi, K.F.; Irié, B.; Dje, C.; Kouamé, G.; Loum, G.; Asseu, O. LCL Filter and Dampers for a Three-Phase, Two-Level Inverter with Six-Pulse Control. *Engineering* **2025**, *17*, 289–314. [CrossRef]
15. Zhang, R.; Chi, S.; Xing, X.; Zhang, C.; Blaabjerg, F. Passivity-based zero-sequence LC resonance suppression method for parallel inverters system with modified LCL filter. *IEEE Trans. Power Electron.* **2025**, *41*, 2618–2628. [CrossRef]
16. Ferrara, C.; Mosca, C.; Cuccia, P.; Urbanelli, A.; Zanghì, A.; Belmonte, L.; Chicco, G. The Role of HVDC Transmission Systems in the Evolution of the Italian Power System. *Energies* **2026**, *19*, 779. [CrossRef]
17. Zafari, L.; Liu, Y.; Ukil, A.; Nair, N.-K.C. Advances in HVDC Systems: Aspects, Principles, and a Comprehensive Review of Signal Processing Techniques for Fault Detection. *Energies* **2025**, *18*, 3106. [CrossRef]
18. Shufian, A.; Hossain, M.I.; Anonto, H.Z.; Rohan, A.I. Enhancing stability in renewable energy transmission using multi-terminal HVDC systems with grid-forming controls for offshore and onshore wind integration. *Sci. Rep.* **2025**, *15*, 42028. [CrossRef] [PubMed]
19. Rifat, M.J.H.; Ghassemi, M. Transmission power grid hardening strategies against hurricane-induced extreme weather conditions: A comprehensive review. *IEEE Access* **2025**, *13*, 61768–61791. [CrossRef]
20. Li, X.; Xie, Z.; Zeng, L.; Zhao, L. Calculation Methods of High-Voltage Direct Current (HVDC) Line Sag Considering Meteorology. *Energies* **2024**, *17*, 305. [CrossRef]

Disclaimer/Publisher's Note: The statements, opinions and data contained in all publications are solely those of the individual author(s) and contributor(s) and not of MDPI and/or the editor(s). MDPI and/or the editor(s) disclaim responsibility for any injury to people or property resulting from any ideas, methods, instructions or products referred to in the content.